12WCEE 2000

0763

A HYBRID METHOD FOR PREDICTING STRONG GROUND MOTIONS AT BROAD-FREQUENCIES NEAR M8 EARTHQAUKES IN SUBDUCTION ZONES

Yoshiaki HISADA[1]

SUMMARY

The near-field strong motions during the 1985 Michoacan earthquake (M8) are successfully simulated at broadband frequencies. For the simulation at low frequencies (0 to 1 Hz), the modified k-square model (Hisada, 1999) is used by considering the k-squared (wavenumber-squared) distributions of slip (Mendoza and Hartzell, 1989) and the incoherent rupture time. For modeling the slip velocity, the Kostrov-type function with fmax of 10 Hz is adopted. The simulated results reproduced well the observed long-period ground motions, including the ramp-function-like displacements with the permanent offsets, and the near-field directivity pulses in the velocities. On the other hand, for the simulation at high frequencies (0.5 to 10 Hz), the Kamae-Irikura-Boore method (Kamae, *et al*, 1998) is used. The results reproduced well the observed accelerations including the directivity effects. Accordingly, the simulated Fourier spectra agree well with those observed at broadband frequencies (0 to 10 Hz). The source parameters of an M8 earthquake in a subduction zone can be easily applied to strong motion predictions in other areas using appropriate Green's functions.

INTRODUCTION

Since the 1994 Northridge and 1995 Hyogoken-Nanbu (Kobe) earthquakes, it is becoming possible to simulate realistic near-field strong motions for M7 earthquakes (e.g., Somerville *et al.*, 1999). However, we still do not have a sound physical model for predicting near-field strong motions at broadband frequencies for M8 earthquakes. This is primarily because we lack good quality strong motion records near earthquakes. On the other hand, it is urgent to predict realistic near-field strong motions for M8 earthquakes in subduction zones, such as, the hypothetical Tokai earthquake, Japan, for disaster prevention.

The purpose of this study is to construct a physical model for predicting near-field strong motions at broadband frequencies for M8 earthquakes. For this, we use a hybrid method: the modified k-square model (Hisada, 1999) at frequencies lower than 1 Hz, and Kamae-Irikura-Boore's stochastic method (Kamae, et al., 1998) at frequencies higher than 1 Hz. We choose the 1985 Michoacan, Mexico, earthquake to construct the source parameters, because the near-field strong motion recorded during this earthquake is probably the only database reliable at broadband frequencies (Figure 1). Somerville et al. (1991) and Dan and Sato (1999) carried out similar strong motion studies using semi-empirical methods.

METHOD

In this study, we combine the two methods: the modified k-square model (Hisada, 1999) at frequencies lower than 1 Hz, and Kamae-Irikura-Boore's method (Kamae, et al., 1998) at frequencies higher than 0.5 Hz.

(A) The Modified K-Square Model for Simulating Long-Period Strong Ground Motions

[1] *Kogakuin University, Dept. of Architecture, Nishi-Shinjuku 1-24-2, Tokyo 163-8677, E-mail: hisada@cc.kogakuin.ac.jp*

The modified k-square model (Hisada, 1999) is a physical omega-square model, which is modified from the k-square model of Bernard et al. (1996) to be more physically appropriate. This model uses a Kostrov-type slip velocity and assumes the k-squared (wavenumber-squared) distributions for the slip and the incoherent rupture time on a fault plane. The displacement in the frequency domain is expressed as follows,

$$U_i(X) = \int_0^L \int_0^W \left\{ \mu \cdot D(e_k n_j + e_j n_k) U^*_{ik,j} \cdot \exp\left(i\varpi \cdot t_r\right) \right\} dxdy \quad \text{.....} \quad (1)$$

where L and W are the fault length and width, μ is the rigidity, D is the slip, e_k and n_j are the slip and fault normal vectors, U^*_{ik} is Green's function, and t_r is the rupture time. For the slip distribution, we use those obtained by source inversion studies.

Regarding the slip velocity function, we use the combination of 6 equilateral triangles (Hisada, 1999) as shown in Figure 2. The slip velocity used in this study has a decay of the inverse of the square root of time (i.e., Kostrov-type: Kostrov, 1964). The minimum duration of the first triangle is 0.1 second, which introduces fmax of 10 Hz as shown in the spectrum in Figure 2.

The rupture time t_r in equation (1) consists of the coherent rupture time (r/Vr) and the incoherent rupture time Δt_r (Figure 3; Hisada, 1999). The coherent rupture time is calculated using the average rupture velocity (Vr), which generates the long-period ground motion. On the other hand, the incoherent rupture time Δt_r generates medium- to high-frequency waves. In order for equation (1) to represent the omega-square model, the spatial wavenumber spectrum of Δt_r has to fall off as the inverse of the wavenumber squared (k-squared: Hisada, 1999). We use the following function as the incoherent rupture time,

$$\Delta t_r(x,y) = \sum_{n=1}^{N} \sum_{m=1}^{M} \frac{4 \cdot \Delta t}{\sqrt{1+(m^2+n^2)^2}} \cos\left(2\pi \cdot m \cdot \frac{x}{L} + \theta_{mn}\right) \cos\left(2\pi \cdot n \cdot \frac{y}{W} + \theta_n\right) \quad \text{.....} \quad (2)$$

where the phases θ_{nm} and θ_n are randomly generated. The lower modes, especially, the first mode (n=m=1) of Δt_r is probably strongly related to the spatial slip variation rather than random distribution. The numerical results for source dynamic by Day (1982) showed that spatial variations of peak slip velocity are strongly coupled to spatial variations of rupture velocity. Since we use the same Kostrov-type slip velocity on the whole fault plane, the slip variations could be directly coupled to those of the rupture velocity. Thus, we calculated Δt_r of the fundamental mode by assuming that the local rupture velocity is proportional to the local slip. The incoherent rupture time used in this study is shown in the bottom of Figure 3, where we used Δt=6 (sec) in equation (2).

(B) Kamae-Irikura-Boore's Method for Simulating Short-Period Strong Ground Motions

To simulate the strong motion at frequencies higher than 1 Hz, we use Kamae-Irikura-Boore's method (Kamae et al., 1998). In this method, we distribute Boore's stochastic point sources (Boore, 1983) on sub-faults in a manner that the total Fourier spectrum follows the omega-square model (Irikura, 1986, Aki, 1972).

BROADBAND STRONG MOTION SIMUTATIONS FOR THE 1985 MICHOACAN EARTHQUAKE

We apply the hybrid method mentioned above to the near strong motions recorded during the 1985 Michoacan earthquake. Figure 1 shows the locations of the fault and the observation stations, CAL (Caleta de Campos), VIL (La Villita), UNI (La Union), and ZIH (Zihuatanejo). We compute the strong motions at the 4 stations using the modified k-square model at frequencies from 0 to 1 Hz, and those using the Kamae-Irikura-Boore method from 0.5 to 10 Hz. Then, we superpose them using the highcut filter for the former (tapering from 0.5 to 1 Hz) and the lowcut filter for the latter (tapering from 1 to 0.5 Hz).

Table 1 shows the structure model used by Somerville *et al*. (1991). Regarding the k-squared model, since we needed to compute about 18,000 Green's functions at each station to express a continuous wavefront, we used the Green's function of the full-space with material properties shown in the bottom of Table 1. Then we multiplied them by the amplification factor using the top two layers. When we compared those results with the results using the complete Green's function of the layered half-space (Hisada, 1995), we found that the waves coming from far sources were overestimated up to about 20%. Therefore, we corrected the amplitudes of the full-space Green functions on the basis of the incident angles. We confirmed that the corrected Green's functions agree well with the complete Green's functions.

Table 2 and 3 show the static source parameters. Those are based on Mendoza and Hartzell (1989), and Somerville *et al.* (1991). Table 4 shows the dynamic source parameters used for the modified k-square model. We use the rupture velocity of 2.8 km/sec to calculate the coherent rupture time. As mentioned above, we compute the fundamental mode of the incoherent rupture time (Δt_r) by assuming that the local rupture velocity on each sub-fault is proportional to the static slip. In our simulations, the max and min local rupture velocities are 3.5 and 1.0 km/s, respectively. For the second and higher modes for Δt_r, we used equation (2) and Δt=6 second. Figure 3 shows the incoherent rupture time. Regarding the slip velocity function, we use afac=$\sqrt{2}$ (the ratio between the areas of subsequent triangles, see Hisada, 1999, and Figure 2). This value makes the decay of the slip velocity to be the inverse of root square of time (i.e., the Kostrov-type function). As shown in Figure 2 and Table 2, we used the fmax=10 Hz and slip duration=3.2 second.

Table 5 shows the source parameters for the Kamae-Irikura-Boore method. For details of those parameters, see Boore (1983) and Kamae *et al.* (1998).

Figures 4 to 6 show the simulated and observed accelerations, velocities, and displacements at the 4 stations. The accelerations are mainly composed of the results by Kamae-Irikura-Boore's method. The directivity effects are well-reproduced; the accelerations near the epicenter show relatively longer duration (CAL and UNI), and those at the forward directivity sites show short duration (UNI and ZIH). Regarding the displacements, the ramp-function-like permanent offsets are also well-represented by the simulations. Accordingly, the corresponding long-period velocity pulses are also reproduced well. These waves are mainly modeled by the slip distribution and the coherent rupture time. On the other hand, the ripples in the velocities are generated mainly by the incoherent rupture time; drastic changes in the rupture front create a series of the near-source long-period pulses. Those features of the observation records are also reproduced well.

Finally, Figure 7 shows the simulated and observed Fourier amplitude spectra. The simulated spectra agree well with those of the observations at broad frequencies.

CONCLUSIONS

We successfully simulated the near-field strong motions during the 1985 Michoacan earthquake at broadband frequencies. For the simulation at frequencies lower than 1 Hz, we adopted the modified k-square model using the k-squared slip distribution by Mendoza and Hartzell (1989) and the k-squared incoherent rupture time. For modeling the slip velocity, we used the Kostrov-type function with fmax of 10 Hz. The simulated results reproduced well the observed long-period ground motions including the ramp-function-like permanent offsets in the displacements (Figure 6) and the near-field directivity pulses in the velocities (Figure 5). On the other hand, for the simulation at frequencies higher than 1 Hz, we used Kamae-Irikura-Boore method. The results reproduced well the observed accelerations including the directivity effects (Figure 4). Accordingly, the simulated Fourier spectra agree with those observed at broadband frequencies (Figure 7). These source parameters can be easily applied to strong motion predictions in the area near a M8 earthquake in a subduction zone.

ACKNOWLEDGEMENTS

This research was partly supported by a special project of "US-Japan Cooperative Research for Urban Earthquake Disaster" by the Ministry of Education, Science, Sports and Culture, and by Disaster Prevention Research Institute of Kyoto University. The advice and discussion with J. Bielak, K. Irikura and K. kamae are greatly improved this research and manuscript.

REFERENCES

Akl, K. (1967), "Scaling Law of Seismic Spectrum", *J. Geophys. Res.*, Vol.72, pp.1217-1231.

Anderson, J.G., *et al.* (1986), "Strong Ground Motion from the Michoacan, Mexico, Earthquake", *Science*, Vol. 233, pp.1043-1049

Bernard, J. A. Herrero, and C. Berge (1996), "Modeling Directivity of Heterogeneous Earthquake Ruptures", *Bull. Seismo. Soc. Am.*, Vol.86, pp.1149-1160.

Boore, D. (1983), "Stochastic Simulation of High-Frequency Ground Motions Based on Seismological Models of Radiated Spectra", *Bull. Seismo. Soc. Am.*, Vol.73, pp.1865-1894.

Dan, K. and T. Sato (1999), "A Semi-Empirical Method for Simulating Strong Ground Motions Based on Variable-Slip Rupture Models for Large Earthquake", *Bull. Seismo. Soc. Am.*, Vol.89, No.1, pp.36-53.

Day, S.M. (1982), "Three-Dimensional Simulation of Spontaneous Rupture: The Effect of Nonuniform Prestress", *Bull. Seismo. Soc. Am.*, Vol.72, No.6, pp.1881-1902.

Hisada, Y. (1995), "An Efficient Method for Computing Green's Function for a Layered Half-Space with Sources and Receivers at Close Depths", *Bull. Seismo. Soc. Am.*, Vol.85, pp.1080-1093.

Hisada, Y. (1999), "A Physical Model for Constructing the Omega-Square Model – Modification of the K-Square Model including Spatial Variation in Slip Distribution, Slip Velocity, and Rupture Velocity –", submitted to *Bull. Seismo. Soc. Am.*

Irikura, K. (1986), "Prediction of Strong Acceleration Motion using Empirical Green's Function", Proc. 7th Japan Earthq. Engng. Sym., pp.151-156

Kamae, K., K. Irikura, and A. Pitarka (1998), "A Technique for Simulating Strong Ground Motion using Hybrid Green's Function", *Bull. Seismo. Soc. Am.*, Vol.88, No.2, pp.357-367.

Kostrov, B.V. (1964), "Self-Similar Problems of Propagation of Shear Cracks", *J. Appl. Math. Mech*., Vol.28, pp.1077-1087.

Mendoza, C. and S. H. Hartzell (1989), "Slip Distribution of the 19 September 1985 Michoacan, Mexico, earthquake: Near-Source and Teleseismic Constraints", *Bull. Seismo. Soc. Am.*, Vol.79, pp655-669.

Somerville, P.G., M. Sen, and B. Cohee (1991), "Simulation of Strong Ground Motions Recorded during the 1985 Michoacan, Mexico and Valparaiso, Chile Earthquakes", *Bull. Seismo. Soc. Am.*, Vol.81, pp.1-27.

Somerville, P. *et al*. (1999), "Characterizing Crustal Earthquake Slip Models for Predicting of Strong Motion", *Seism. Res. Lett.*, Vol.70, pp.59-80.

Table 1: The layered structure model for the Michoacan area (after Somerville *et al*. 1991)

ρ(g/cm3)	Vp(km/s)	Qp	Vs(km/s)	Qs	Thickness (km)
2.50	4.6	200.0	2.7	100.0	0.4
2.68	5.8	200.0	3.4	100.0	5.6
2.78	6.4	200.0	3.7	100.0	-

Table 2: The static source parameters (after Mendoza and Hartzell, 1989)

length (km)	hypocenter along strike (km)		hypocenter along dip (km)	deepest edge (km)
175.0	125.0		90.0	45
width (km)	Strike (deg)	dip(deg)	rake (deg)	Seismic Moment (dyne-cm)
140.0	295.0	14.0	70.0	1.48×10^{28}

Table 3: The Slip Distributions for the 1985 Michoacan Earthquake (after Mendoza and Hartzell, 1989; Somerville *et al*. 1991). The size of subfaults is 25 x 20 km2, and the bottom left of the table corresponds to the northeast of the fault plane (see Figure 1).

1.0	1.6	1.8	1.5	1.4	1.5	0.5
2.5	3.5	1.5	4.0	5.0	3.0	0.5
3.0	4.0	1.7	1.5	3.0	2.5	0.8
2.1	2.5	0.7	1.0	1.3	1.5	0.5
0.8	1.5	1.0	0.7	0.7	1.0	0.5
0.8	2.0	1.7	1.1	0.8	0.5	0.8
1.3	1.3	1.3	0.9	0.8	0.7	1.2

Table 4: The dynamic source parameters for simulating the ground motions during the Michoacan Earthquake using the modified k-squared model (Hisada, 1999)

Coherent V_r (km/s)	Max Vr (km/s)	Min Vr (km/s)	Δt (s)	afac	fmax (Hz)	Slip duration (sec)	N and M in eq.(2)	Green func. per sub- fault
2.8	3.5	1.0	6.0	1.414	10.0	3.2	62	19 x 19

Table 5: The dynamic source parameters for simulating the ground motions during the Michoacan Earthquake using the Kamae-Irikura-Boore's method (Kamae et al., 1998)

Δσ (bar)	fmax (Hz)	$R_{\theta\phi}$	P_{RTITN}	V_r (km/s)
100	10.0	0.63	1/1.414	2.8

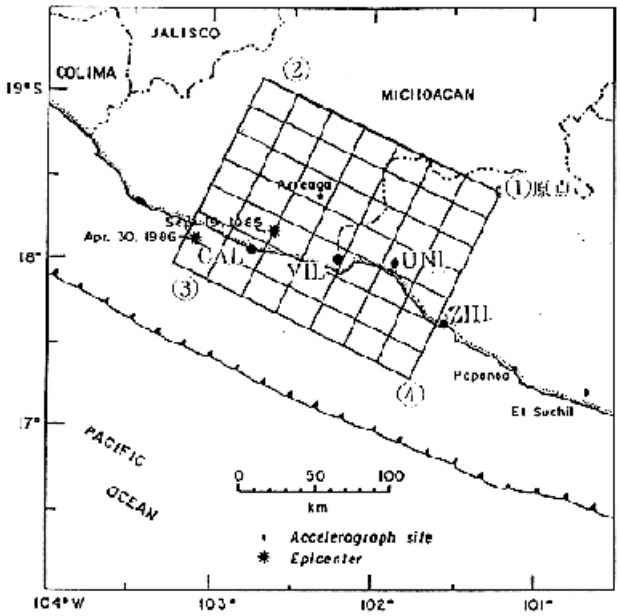

Figure 1. Geographic map of the Michoacan coast showing the surface projection of the fault (175 km x 140 km with the dip angle of 14 degree) used in this study. The fault plane is divided into 7 x 7 sub-faults. The earthquake epicenter and the four strong motion stations are also indicated (after Somerville *et al.*, 1991).

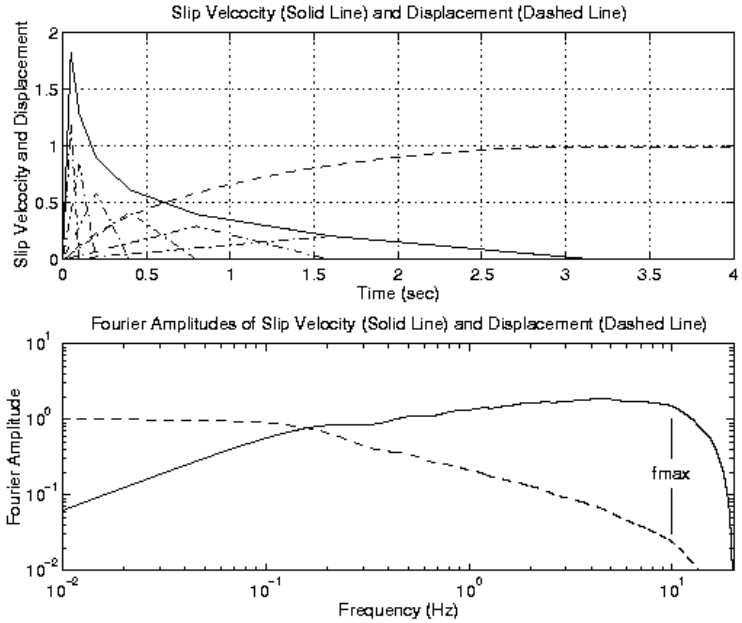

Figure 2. Waveforms (Top) and their Fourier Spectra (Bottom) of the slip velocity and displacement used in this study. The slip velocity consists of 6 equilateral triangles with different durations (0.1, 0.2, 0.4, 0.8, 1.6 and 3.2 seconds), as shown in the dashed and dotted lines in the top figure. Its amplitude decays as the inverse of the square root of time (i.e., the Kostrov-type function). The minimum duration of the first triangle is 0.1 second, and it creates the fmax of 10 Hz as shown in the spectra.

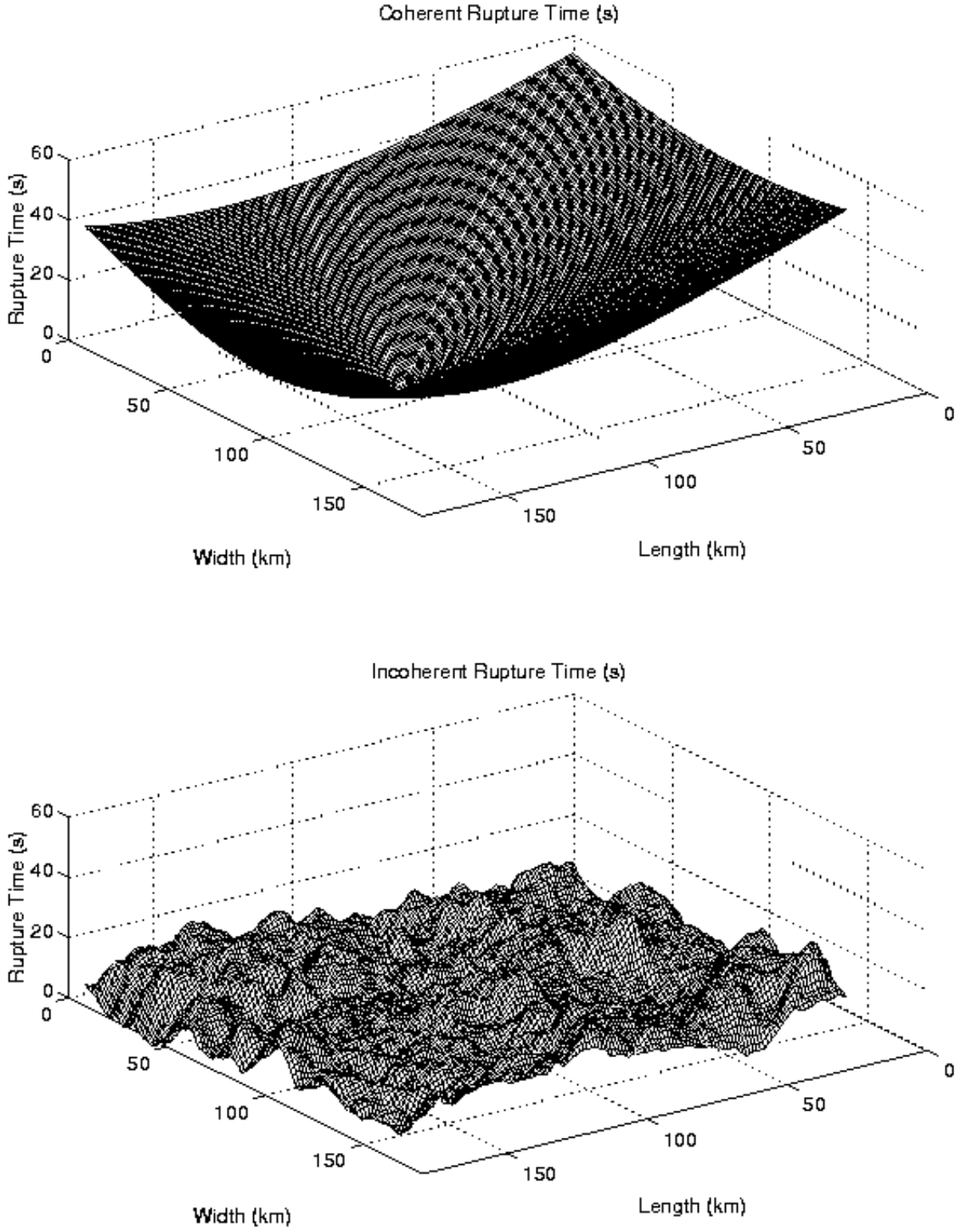

Figure 3. The coherent rupture time (top) and the incoherent rupture time (bottom) on the fault plane of the 1985 Michoacan earthquake model, viewing from the southwest edge to the northeast edge). Equation (2) and the values of Table 4 are used. The wavenumber spectrum amplitude of the distribution of the incoherent rupture time (bottom) falls of as the inverse of wavenumber squared.

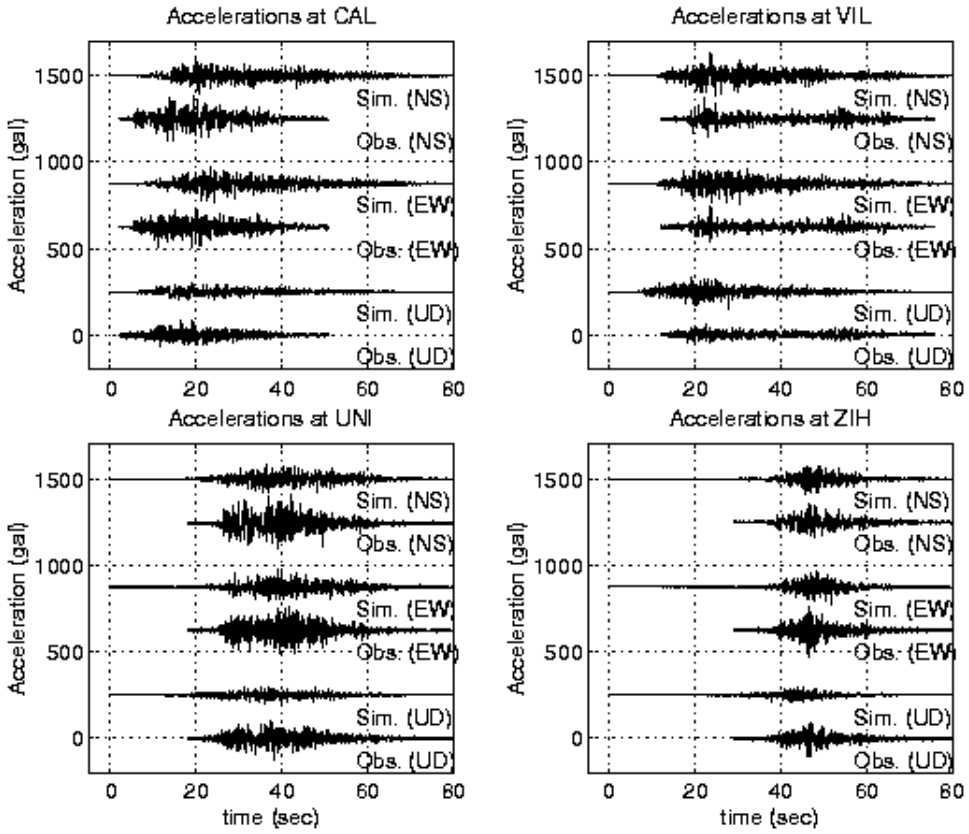

Figure 4. Simulated and observed accelerations at the four stations, CAL, VIL, UNI, and ZIH.

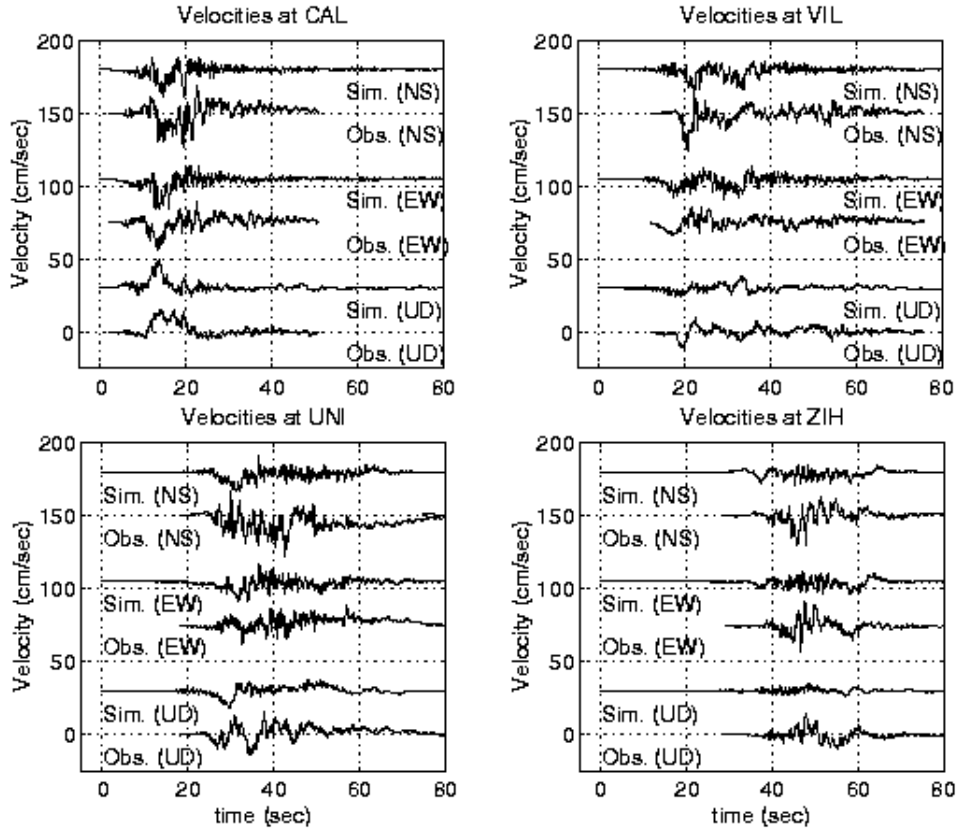

Figure 5. Simulated and observed velocities at the four stations, CAL, VIL, UNI, and ZIH.

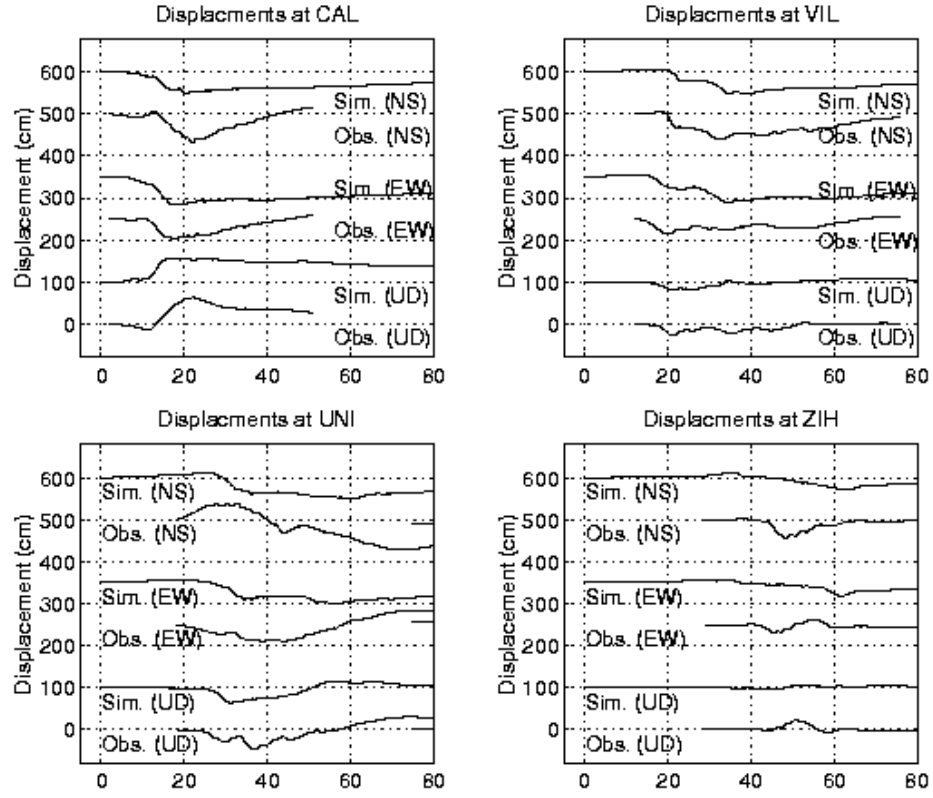

Figure 6. Simulated and observed displacements at the four stations, CAL, VIL, UNI, and ZIH.

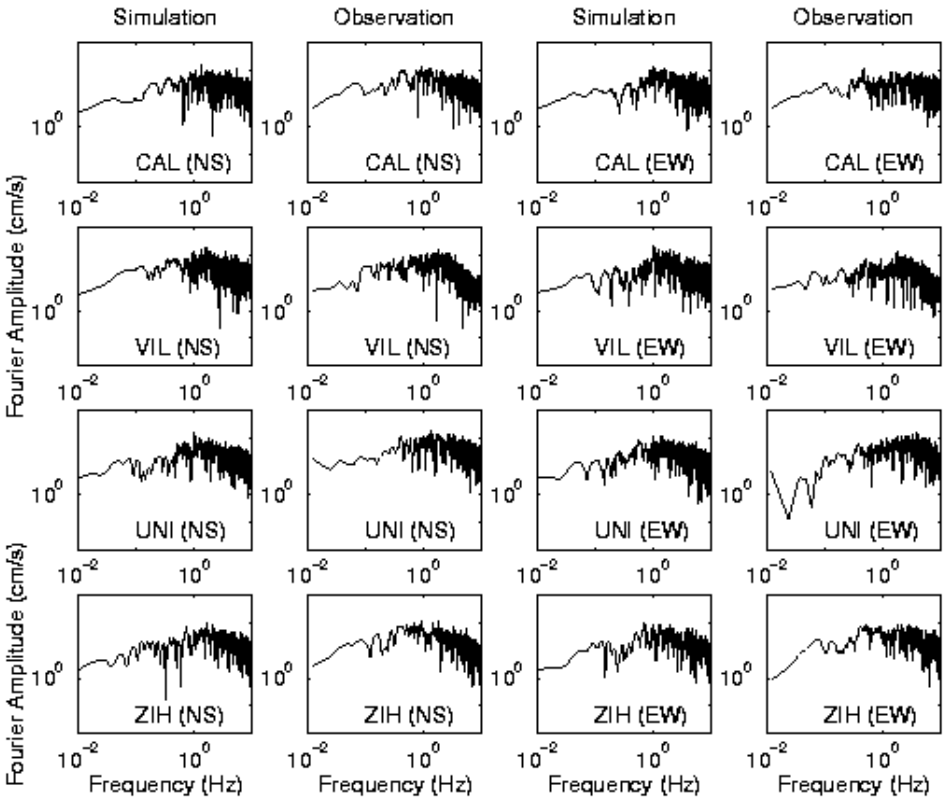

Figure 7. Simulated and observed Fourier acceleration spectra from 0.01 to 10 Hz at the four stations